ELSEVIER

Journal of Alloys and Compounds 434–435 (2007) 56–59

Journal of ALLOYS AND COMPOUNDS

www.elsevier.com/locate/jallcom

Glass forming ability and mechanical properties of the NiZrTiSi amorphous alloys modified with Al, Cu and Nb additions

Tomasz Czeppe [a,*], Patrick Ochin [b], Anna Sypień [a]

[a] *Institute of Metallurgy and Materials Science PAS, Reymonta 25 Street, 30-059 Kraków, Poland*
[b] *Centre d'Etudies de Chimie Métallurgique, UPR-CNRS no. 2801, 15, rue G. Urbin, 94400 Vitry/Saine, France*

Available online 17 October 2006

Abstract

The composition of the amorphous alloy $Ni_{59}Zr_{20}Ti_{16}Si_5$ was modified with 2–9 at.% additions of Cu, Al and Nb. The ribbons and the bars 2.7 mm in diameter were prepared by melt spinning and injection casting from the alloys of the compositions: $Ni_{56}Zr_{18}Ti_{16}Si_5Al_3Cu_2$, $Ni_{56}Zr_{18}Ti_{13}Al_6Si_5Cu_2$, $Ni_{56}Zr_{16}Ti_{12}Nb_9Al_3Cu_2Si_2$ and $Ni_{56}Zr_{16}Ti_{12}Nb_6Al_6Cu_2Si_2$. All ribbons were amorphous up to the resolution of the X-ray diffraction and conventional transmission electron microscopy, however rods were partially crystalline. Increase of Al content lowered and Nb content slightly increased crystallization start temperature T_x and glass transition temperature T_g. The influence of composition changes on the overcooled liquid range ΔT was more complicated. The increase of Nb and decrease of Ti and Zr content led to the remarkable increase of the liquidus temperature T_l. As a result GFA calculated as T_g/T_l was lowered to the values about 0.63 for 6 and 9 at.% Nb addition. The activation energies for primary crystallization in alloy with 6 at.% Al and 6 at.% of Nb, were determined. The changes of tensile test strength and microhardness with Al and Nb additions showed hardening effect caused by Nb additions and increase in fracture strength with increasing Al content.

Keywords: Metallic glasses; Rapid-solidification; Mechanical properties; Transmission electron microscopy; Thermal analysis

1. Introduction

The interest in Ni–Ti–Zr amorphous alloys led to develop some families of Ni-based alloys with non-metallic additions like P, B or Si and high glass forming ability (GFA) [1,2]. Ni, Ti, Zr and Si fulfill known empirical rules for the glass formers since both Ni–Ti and Ni–Zr alloys form deep eutectics, the differences between atomic radii of Ti(Zr) and Ni exceeds 18% and enthalpy of mixing of these elements with Si is large and negative [2]. The systematic studies under the optimization of the compositions show that a few percent additions of Sn may improve GFA [3], while Nb, Co Cr, Mo and Cu additions may increase ΔT range of supercooled liquid as well as the strength and corrosion resistance of the alloys [4–6]. The Al addition promotes lower temperature of crystallization [7]. The Si addition increases GFA, glass transition and crystallization temperatures [2] but may lower mechanical properties of the alloys [4,5]. One of the compositions leading to the amorphous, 2 mm in diameter BMG was $Ni_{59}Zr_{20}Ti_{16}Si_5$ [1], revealing glass transition (T_g) at temperature 830 K, first crystallization at 876 K and supercooled liquid range 46 K (defined as an onset point). The investigation of the Nb component influence of the amorphous alloys showed enhanced strength and a plastic deformation range in compression test as well as increase in characteristic temperatures [8]. In the present work this composition was modified with 2–9 at.% additions of Cu, Al and Nb. The properties of the $Ni_{56}Zr_{18}Ti_{16}Si_5Al_3Cu_2$, $Ni_{56}Zr_{18}Ti_{13}Al_6Si_5Cu_2$, $Ni_{56}Zr_{16}Ti_{12}Nb_9Al_3Cu_2Si_2$ and $Ni_{56}Zr_{16}Ti_{12}Nb_6Al_6Cu_2Si_2$ alloys were investigated. The earlier results concerning first of this alloys were presented in [9].

2. Experimental

The chemical compositions of the investigated alloys are presented in Table 1. The alloys were prepared from a high purity components by melting in a Balzers furnace under an argon atmosphere and cast in an iron chill mould of the 20 cm^3 volume, in vacuum. The samples were prepared by melting in quartz crucibles and spun on the CuCoBe rotating disc 20 cm in diameter. The 19 m/s linear velocity of the disc and 150–180 mbar pressure of He gas were used. The ribbons 9 mm in width and of 50 μm thickness were achieved. The massive samples in the form of bars of the diameter 2.7 mm were prepared by injection casting into the copper mould.

* Corresponding author. Tel.: +48 12 637 42 00.
E-mail addresses: nmczeppe@imim-pan.krakow.pl (T. Czeppe), patrickochin@glut-cnrs.fr (P. Ochin), nmsypien@imim-pan.krakow.pl (A. Sypień).

0925-8388/$ – see front matter © 2006 Elsevier B.V. All rights reserved.
doi:10.1016/j.jallcom.2006.08.327

The chemical composition of the alloys was controlled by the EDX analysis system with the scanning electron microscope (SEM) Philips XL 30. The phase analysis was performed by X-ray diffractometry with the Philips PW 1830 diffractometer. The microstructure of the ribbons was studied with the use of transmission electron microscope Philips CM20 (200 kV) equipped with the EDAX Phoenix system. Thermal analysis was performed with the use of TA DSC Q1000 and SDT Q600 calorimeters. Glass transition temperature was defined as the inflection point on the DSC curves.

Tensile test was performed with the INSTRON 6025 and Zeiss microhardness tester with the 20 G load was applied for to estimate microhardness on the ribbons cross-sections. No less than 10 indentations were made for each average value of the Vickers microhardness on different parts of the ribbon samples.

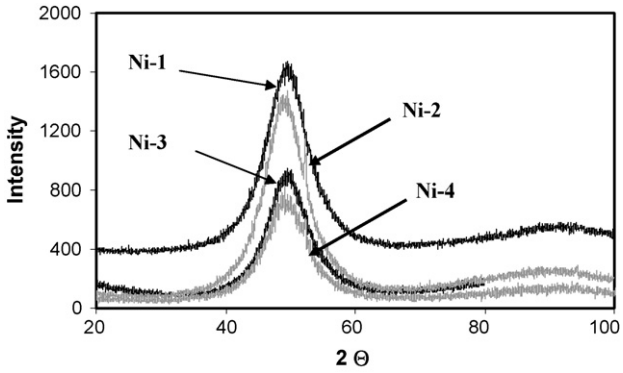

Fig. 1. X-ray patterns of the ribbons (Cu Kα radiation applied).

3. Results and discussion

3.1. Microstructure of the ribbons

All ribbons reveal amorphous microstructure both investigated by X-ray diffraction and TEM, however all the massive bars, analyzed by X-ray diffraction only, were partially crystalline. The X-ray diffraction patterns are presented in Fig. 1. The TEM electron diffractions and dark field microstructures are presented in Fig. 2a–d.

3.2. Thermal analysis of the ribbons

DSC thermal analysis is presented in Fig. 3 and characteristic temperatures are summarized in Table 1. The Ni-1 ribbon revealed the highest crystallization temperature, while the Ni-4 the lowest. The thermal effect of crystallization in both cases is singular. In spite of the different composition ribbons Ni-2 and Ni-3 revealed very similar crystallization temperatures. The crystallization of this ribbons proceeded in two separated stages. Glass transition temperature (T_g) was clearly visible for all but Ni-4 alloy. T_g decreased after increasing Al and decreasing Ti and Zr content in alloy Ni-2, was not changed after similar replacing Al, Zr, Ti and Si by 9 at.% of Nb in alloy Ni-3 but was lowered by the decrease of Nb content in alloy Ni-4. The analysis of this results show that the increase in Al addition decreases both T_g and T_x temperatures when Nb addition acts opposite but rather weakly. Larger content of Zr, Ti and Si strongly increases both temperatures. All investigated alloys melted in one thermal

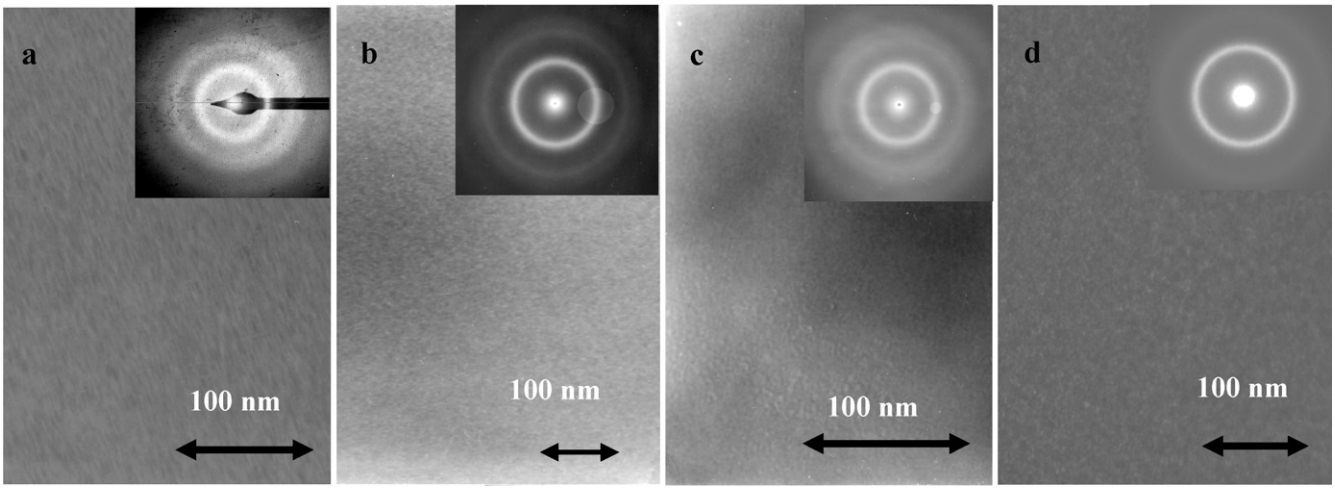

Fig. 2. Transmission electron microscopy of the ribbons: (a) Ni-1, (b) Ni-2, (c) Ni-3 and (d) Ni-4.

Table 1
Chemical composition of the alloys and results of thermal analysis

Alloy	Chemical composition	T_g (K)	T_x (K)	T_{melt} (K)	T_l (K)	ΔT (K)	$T_x/(T_g + T_l)$	T_g/T_l
Ni-1	$Ni_{56}Zr_{18}Ti_{16}Si_5Al_3Cu_2$	846	875	1250	1256	29	0.42	0.67
Ni-2	$Ni_{56}Zr_{18}Ti_{13}Al_6Si_5Cu_2$	831	860	1248	1250	29	0.41	0.67
Ni-3	$Ni_{56}Zr_{16}Ti_{12}Nb_9Al_3Cu_2Si_2$	831	863	1302	1312	32	0.40	0.63
Ni-4	$Ni_{56}Zr_{16}Ti_{12}Nb_6Al_6Cu_2Si_2$	810	834	1285	1298	24	0.40	0.62

Values of T_g measured at the rate 0.33 K/s and defined as an inflection point, T_{melt} and T_l measured at the rate 0.05 K/s.

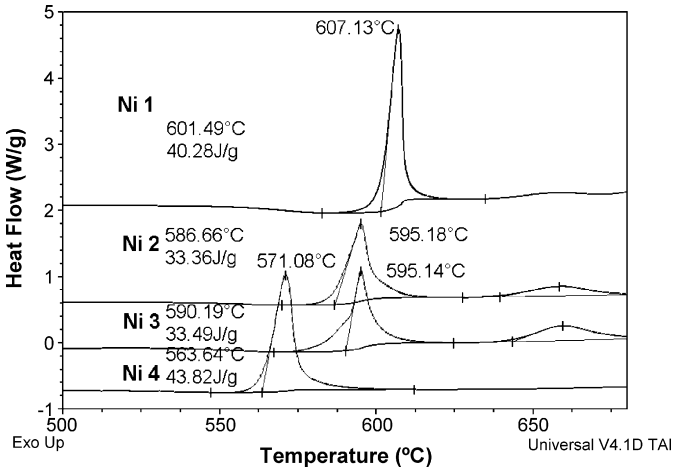

Fig. 3. DSC thermal curves for the investigated alloys; heating rate 0.33 K/s.

effect suggesting near to eutectic compositions but Nb addition increases T_{liq}–T_{sol} interval. The melting temperature and temperature of liquidus, determined from the peak temperatures were slightly lowered for the alloy Ni-2 and remarkably increased for alloys Ni-3 and Ni-4 with Nb additions. Neither increase of Al content nor that of Ti, Zr and Si additions influenced T_m remarkably, but Nb addition increased it. Overcooled liquid range ΔT remained not sensitive for Al content changes but increased in case of Ni-3 alloy with 9 at.% Nb content, what however is rather a result of the determining T_x temperature as the onset of the main crystallization peak (Fig. 3). As a result of a stronger influence of Nb addition on liquidus temperature T_l, T_g/T_l value was lowered for alloys Ni-3 and Ni-4. If GFA is defined as $T_x/(T_g + T_l)$ [10] it remains lowered but practically constant for the Nb containing alloys. Values of T_g, ΔT, T_{sol}, T_l, $T_x/(T_g + T_l)$ and T_g/T_l are presented in Table 1.

Activation energy for the crystallization was determined for the Ni-1 and Ni-4 alloys by Kissinger method [11] for the constant heating rates, from 5 to 50 K/min (Fig. 4). As a result the values of 385 kJ/mol for alloy Ni-1 and 427 kJ/mol for alloy Ni-4 were estimated.

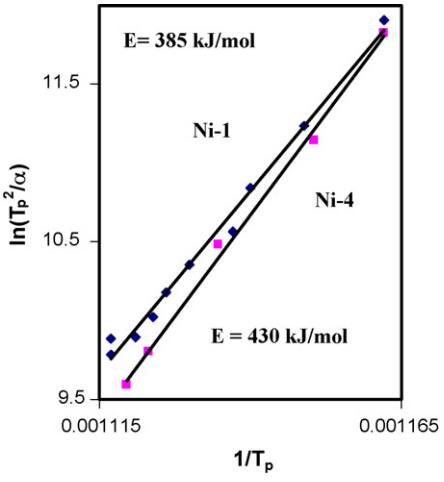

Fig. 4. The activation energy for the primary crystallization for the Ni-1 and Ni-4 alloys determined with the Kissinger method.

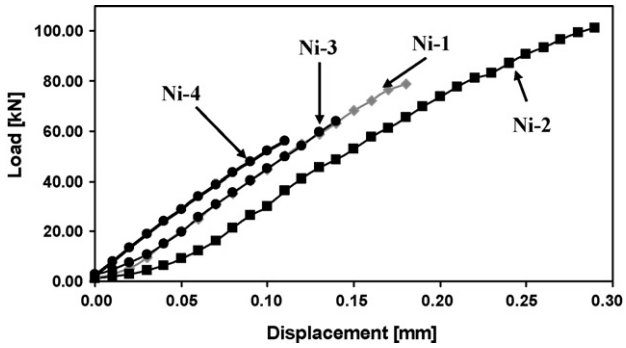

Fig. 5. Tensile test results for the investigated ribbons. Applied velocity of the machine traverse was 8.4×10^{-4} mm/s.

3.3. Mechanical properties and microhardness

The tensile test was performed on the ribbons (Fig. 5). Both ribbons Ni-3 and Ni-4 containing Nb and less Ti and Zr, revealed smaller fracture strength, 711 and 633 MPa, respectively, than Ni-1 ribbon (866 MPa) in an amorphous state. A highest fracture strength, 1122 MPa, in the elastic deformation range, showed the Ni-2 ribbon with the highest Al and 5 at.% Si content.

The microhardness of ribbons Ni-1, Ni-2 and Ni-3 was similar, in the range of 920–990 (±160) μHV. The microhardness of the ribbon Ni-4 was somehow smaller, in the range of 780 (±100) μHV. The result suggests that Nb addition increases hardness but less than the decrease of the Ti, Zr and Si content lowers it.

4. Conclusions

1. Melt spun ribbons from alloys of composition $Ni_{56}Zr_{18}Ti_{16}Si_5Al_3Cu_2$, $Ni_{56}Zr_{18}Ti_{13}Al_6Si_5Cu_2$, $Ni_{56}Zr_{16}Ti_{12}Nb_9Al_3Cu_2Si_2$ and $Ni_{56}Zr_{16}Ti_{12}Nb_6Al_6Cu_2Si_2$ revealed amorphous structure while the bars 2.7 mm in diameter were partially crystalline.
2. Three atomic percent addition of Al lowers T_g and T_x temperatures without remarkable influence on the melting temperature. It decreased microhardness and increased tensile strength of the ribbons.
3. Nb additions weakly increase glass transition and crystallization temperatures and to a greater extent melting temperature, leading to the lowered T_g/T_l and GFA values.
4. Nb additions lead to the hardening of the alloy and lowered the tensile strength of the ribbons.
5. The activation energy for the primary crystallization, determined for $Ni_{56}Zr_{16}Ti_{12}Nb_6Al_6Cu_2Si_2$ alloy is slightly higher than for the crystallization of the cubic NiTi(Zr) in case of the $Ni_{56}Zr_{18}Ti_{16}Si_5Al_3Cu_2$ alloy.

Acknowledgements

The work was supported by the Polish Ministry of the Science and Information Society Technologies as the Project No. 3 T08A 067 28. Financial support from the European Union (Project MCRTN-CT-2003-504692) is gratefully acknowledged.

References

[1] J.K. Lee, S.H. Kim, S.H. Yi, W.T. Kim, D.H. Kim, Mater. Trans. 42 (2001) 592–596.
[2] S. Yi, J.K. Lee, W.T. Kim, D.H. Kim, J. Non-Cryst. Solids 291 (2001) 132–136.
[3] J.K. Lee, D.H. Bae, W.T. Kim, D.H. Kim, Mater. Sci. Eng. A 375–377 (2004) 332–335.
[4] T. Zhang, A. Inoue, Mater. Trans. 43 (4) (2002) 708–711.
[5] S. Pang, T. Zhang, K. Asami, A. Inoue, Mater. Trans. 43 (7) (2002) 1771–1773.
[6] X. Wang, I. Yoshii, A. Inoue, Y.H. Kim, I.B. Kim, Mater. Trans. JIM 40 (10) (1999) 1130–1136.
[7] M.H. Lee, W.T. Kim, D.H. Kim, Y.B. Kim, Mater. Sci. Eng. A 375–377 (2004) 336–340.
[8] A. Inoue, W. Zhang, T. Zhang, Mater. Trans. 43 (2002) 1952–1956.
[9] T. Czeppe, E. Vassileva, J. Dutkiewicz, in: K.J. Kurzydłowski, Z. Pakieła (Eds.), Bulk and Graded Nanomaterials, Trans. Tech. Publ., Switzerland, Solid State Phenom., 101–102 (2005) 241–246.
[10] Z.P. Lu, C.T. Liu, Acta Mater. 50 (2002) 3501–3512.
[11] H.E. Kissinger, Anal. Chem. 29 (1957) 1702.